# Finite element simulations of clayey soil ground with a three-dimensional nonlinear elastic viscoplastic model

**Ze-Jian Chen[1,*], Wei-Qiang Feng[1] and Jian-Hua Yin[1]**

[1] Department of Civil and Environmental Engineering, The Hong Kong Polytechnic University

Hong Kong SAR, China

ze-jian.chen@connect.polyu.hk

**Abstract** This paper presents a study on numerical simulations of clayey soil using nonlinear elastic viscoplastic (EVP) model. The nonlinear EVP model is based on Yin (1999)'s nonlinear creep equation in which a creep strain limit is considered. The model in the general stress-strain condition is implemented by finite element program Plaxis and is used to simulate clayey soil under Berthierville embankment. Good agreement between simulated and measured settlements and excess pore pressure validates the feasibility of the nonlinear EVP model. Furthermore, a parametric study is presented to demonstrate the importance of creep strain limit.

**Keywords**: clayey soil; creep; elastic viscoplastic; finite element simulation; settlement

## 1 Introduction

The rheology of soft clayey soils has been widely recognized by researchers and engineers in the past decades, which has significant effects on the deformations of soft soil ground. Rheology is performed through different kinds of time-dependent behaviours of clayey soils, including creep, stress relaxation and rate-dependent deformation behaviours. These properties might result in severe engineering problems such as excessive long-term settlements, reduction of soil stability, etc. Consequently, proper constitutive modelling and calculation method for clayey soils is needed. A series of rheology models for clayey soils have been proposed since last century, based on the phenomena of creep and strain rate dependency. Bjerrum (1967) introduced a series of "time line" parallel to the conventional compression curves for describing the creep behaviours of soils. Yin and Graham (1989) introduced the concept of "equivalent time" into the creep model and developed an elastic viscoplastic (EVP) model for soft clays. Many of the existing rheology models adopt constant correlations with logarithmic scale of time which lead to infinitely increasing creep strain with increase of time, which obviously violates the natural rule. Therefore, a nonlinear creep equation was proposed by Yin (1999) to consider the creep strain limit, which has been developed into a 3-D constitutive model later by Yin et al. (2002) based on the overstress theory (Perzyna, 1966) and modified Cam-Clay model, as shown in Fig. 1.

This study introduces the implementation of a 3-D nonlinear EVP model in Plaxis for finite element analysis. The model is then used to simulate the deformation of the clayey soil under Berthierville embankment, and the results are compared with measured data. A parametric study is also carried out on the effects of creep strain limit.

## 2 Equations and numerical implementation of the EVP model

### *2.1 The 3-D elastic viscoplastic model based on creep equations*

In the $\varepsilon - \ln\sigma'$ plane, there exists a unique relationship among $\dot{\varepsilon}^{vp}$ (or $t_e$), $\sigma'$ and $\varepsilon$, forming a series of time lines, as shown in Fig. 1. According to the nonlinear equation by Yin (1999), the 1-D viscoplastic strain rate is expressed as:

$$\dot{\varepsilon}^{vp} = \frac{\mathrm{d}\varepsilon^{vp}}{\mathrm{d}t} = \frac{\psi_0}{Vt_0}\exp\left[\frac{-V\Delta\varepsilon^{vp}}{\psi_0\left(1-\dfrac{\Delta\varepsilon^{vp}}{\Delta\varepsilon_L}\right)}\right]\left(1-\frac{\Delta\varepsilon^{vp}}{\Delta\varepsilon_L}\right)^2 \tag{1}$$

where $\Delta\varepsilon^{vp}$ is the creep strain deviated from the reference line ($\lambda$-line), $\psi_0$ is the initial creep coefficient and $\Delta\varepsilon_L$ is the creep strain limit.

For the general stress-strain condition, the invariants of mean effective stress $p'$ and deviatoric stress $q$ are adopted in the framework, as shown in Eqs. (2) and (3)

$$p' = \frac{tr\left(\sigma'_{ij}\right)}{3} = \frac{\sigma'_{11}+\sigma'_{22}+\sigma'_{33}}{3} \tag{2}$$

$$q = \sqrt{\frac{3}{2}\left(s_{ij}\cdot s_{ij}\right)} \tag{3}$$

where

$$s_{ij} = \sigma'_{ij} - \delta_{ij}p'$$
$$\text{Kronecker delta} \quad \delta_{ij} = \begin{cases} 1 & i=j \\ 0 & i\neq j \end{cases} \tag{4}$$

According to the overstress theory, the strain rate is divided into elastic and viscoplastic parts ($\dot{\varepsilon}_{ij} = \dot{\varepsilon}_{ij}^{vp} + \dot{\varepsilon}_{ij}^{e}$), determined from Eqs. (5) and (6) respectively:

$$\dot{\varepsilon}_{ij}^{e} = D_{ijkl}\dot{\sigma}_{ij}^{e} \qquad k=1,2,3 \text{ and } l=1,2,3 \tag{5}$$

$$\dot{\varepsilon}_{ij}^{vp} = \gamma\left\langle\phi(F)\right\rangle\frac{\partial f}{\partial\sigma_{ij}} = S\frac{\partial f}{\partial\sigma_{ij}} \tag{6}$$

where $f$ is the load potential function and $f$=0 is similar to the concept of yield surface in modified Cam-Clay model. $S$ is a scaling function to replace $\gamma\langle\phi(F)\rangle$ to describe the position of yield surface (Yin et al., 2002). Therefore, $\dot{\varepsilon}_{ij}$ can be expressed by

$$\dot{\varepsilon}_{ij}=\left(\frac{1}{2G^e}\dot{s}_{ij}+\frac{\dot{p}'}{3K^e}\dot{\delta}_{ij}\right)+S\frac{\partial f}{\partial\sigma'_{ij}} \tag{7}$$

where $K^e=\dfrac{Vp'}{\kappa}$ and $G^e=\dfrac{2(1-2\nu)K^e}{2(1+\nu)}$, $\kappa$ is the slope of re-loading line in the $e-\ln p'$ plane, $\nu$ is the Poisson's ratio, $V$ is the initial specific volume and $V$=1+$e_0$.

The loading potential surface controls the flow direction of time-dependent strain, as shown in Fig. 1. A loading potential function $f$ that is able to consider anisotropy is adopted (Yin et al., 2010):

$$f=\frac{3\left(s_{ij}-p'\alpha_{ij}\right):\left(s_{ij}-p'\alpha_{ij}\right)}{2\left(M^2-\frac{3}{2}\alpha_{ij}:\alpha_{ij}\right)p'}+p'-p'_m \tag{8}$$

where $M$ is the slope of critical line in the $p'-q$ plane, and $\alpha_{ij}$ is the deviatoric fabric tensor. When $\alpha_{ij}$=0, $f$ can be reduced into the loading potential surface in modified Cam-Clay model. $p'_m$ represents the size of loading potential surface under current stress-strain state. In Fig. 1, $p'_m$ is the intersection of loading surface $f$=0 and the $p'$ axis, at which the soil is under isotropic stress state. To determine the value of $S$ under general stress-strain condition, the following equation can be used according to Eq. (6):

$$S=\frac{\dot{\varepsilon}_v^{vp}}{\left|\dfrac{\partial f}{\partial p'}\right|} \tag{9}$$

where $\dot{\varepsilon}_v^{vp}$ is the viscoplastic volumetric strain rate. As shown in Fig. 1, it is assumed that the volumetric viscoplastic strain rate under current stress-strain state is equal to that under isotropic effective stress $p'_m$ within the same yield surface, and therefore can be derived from the 1-D EVP model as:

$$\dot{\varepsilon}_v^{vp}=\dot{\varepsilon}_{vm}^{vp}=\frac{\psi_0}{Vt_0}\left(1+\frac{\left(\varepsilon_{vm}^r-\varepsilon_{vm}\right)}{\Delta\varepsilon_L}\right)^2\exp\left\{\frac{V\left(\varepsilon_{vm}^r-\varepsilon_{vm}\right)}{\psi_0\left[1+\dfrac{\left(\varepsilon_{vm}^r-\varepsilon_{vm}\right)}{\Delta\varepsilon_L}\right]}\right\} \tag{10}$$

The corresponding strain state $\varepsilon_{vm}$ and reference strain state $\varepsilon_{vm}^r$ is determined from isotropic compression curves using the following equations respectively:

$$\varepsilon_{vm}=\varepsilon_v+\frac{\kappa}{V}\ln\frac{p'_m}{p'} \tag{11}$$

$$\varepsilon_{vmr} = \varepsilon_{vmr0} + \frac{\lambda}{V} \ln \frac{p'_m}{p'_{mr0}} \tag{12}$$

where $\kappa$ is the slope of re-loading line in the $e - \ln p'$ plane, $\lambda$ is the slope of normally consolidation line in the $e - \ln p'$ plane, and ($\varepsilon_{vmr0}$, $p'_{mr0}$) is a fixed point on the reference line, which is relevant to the initial pre-consolidation pressure.

### *2.2 Algorithm scheme of implementation in Plaxis for the EVP model*

In this study, the EVP model is encoded in Plaxis 2017 by the "user-defined soil model" modulus using Fortran language. For each calculation step on each node, the user-defined model receives the stress-strain state from last step from Plaxis and returns with a new stress after calculation. Sub-steps can be produced, the number of which is controlled by the directly input parameter named Step size, or by the largest strain step which is set as 1/10000 in this study. The calculation is achieved by a Newton-Raphson iteration procedure, briefly introduced as follows.

The increase of effective stress is contributed by the elastic strain increment, as indicated by:

$$\begin{aligned} \sigma^{n+1} &= \sigma^n + \Delta\sigma^n \\ &= \sigma^n + D^{-1} \cdot \left(\Delta\varepsilon^n - \Delta\varepsilon^{vp,n}\right) \end{aligned} \tag{13}$$

The strain increment adopted Euler time integration scheme, which is a combination of explicit and implicit methods:

$$\Delta\varepsilon^{vp,n} = \Delta t \cdot \left[(1-\theta) \cdot \Delta\dot{\varepsilon}^{vp,n} + \theta \cdot \Delta\dot{\varepsilon}^{vp,n+1}\right] \tag{14}$$

where $\theta$ is used to adjust the Euler integration. $\theta$ varying from 0 to 1 represent fully explicit to fully implicit analysis. Therefore, Eq. (13) can be expressed by:

$$D \cdot \sigma^{n+1} + \Delta t \cdot \theta \cdot \Delta\dot{\varepsilon}^{vp,n+1} = \Delta\varepsilon^n - \Delta t \cdot (1-\theta) \cdot \Delta\dot{\varepsilon}^{vp,n} + D \cdot \sigma^n \tag{15}$$

The unknown left side of Eq. (15) is calculated by Newton-Raphson iteration, in which a limited Taylor's series about a trial stress $\sigma^i$ is used:

$$\begin{cases} \sigma^{n+1} = \sigma^i + d\sigma^i \\ \dot{\varepsilon}^{vp,n+1} = \dot{\varepsilon}^{vp,i} + \dfrac{\partial \dot{\varepsilon}^{vp,i}}{\partial \sigma} d\sigma \end{cases} \tag{16}$$

The above equations yield an equation in matrix forms:

$$d\sigma^i = \left[\frac{\partial G}{\partial \sigma}\right]^{-1} \cdot \left[Q^n - G^i\right] \tag{17}$$

Details of $Q$ and $G$ can be found in Feng et al. (2014). Iterations will be conducted until the stress increment $d\sigma^i$ reaches a tolerance criterion. For undrained condition, the excess pore pressure should be updated and returned to the consolidation analysis for the next step:

$$u^{n+1} = u^n + d\varepsilon_v^{n+1} \cdot K_w \tag{18}$$

where $K_w$ is the bulk modulus of the water.

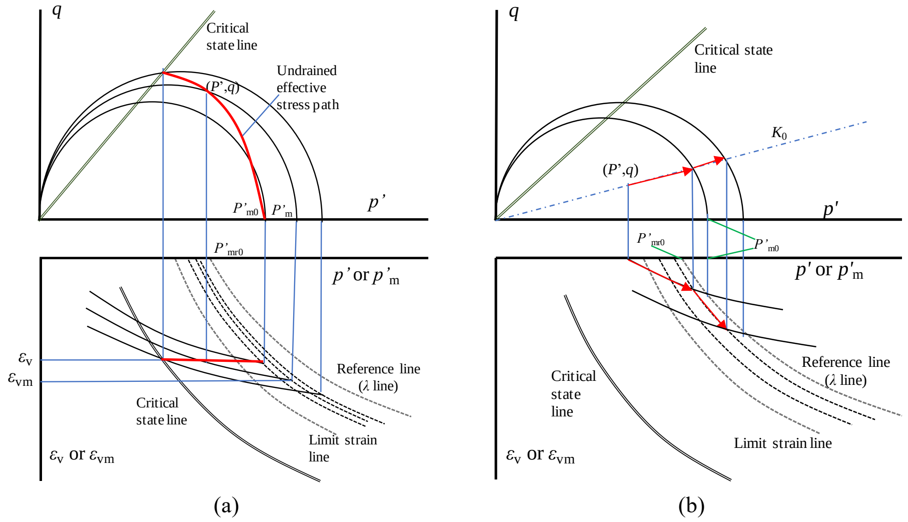


**Fig.** 1 The schematic diagram of the nonlinear EVP model for (a) CU tests and (b) oedometer tests

## 3 Simulations on Berthierville embankment using the EVP model

### *3.1 Simulated settlements and excess pore pressure of the Berthierville clay*

The Berthierville embankment was constructed in a field in Canada, where the soil ground consisted of multi-layers of clay, silt and sand and there exists a thick layer of silty clay in the upper parts. The clay was located between a middle to fine sand layer and a silty sand layer and can be regarded as two-way drained system. The detailed parameters can be found in Tables 1 and 2, according to published literature (Kabbaj et al., 1988). The compression index $\lambda$ and $\kappa$ are fitted by 24-h multi-stage-loading consolidation curves. The creep coefficient $\psi_0$ and $\Delta\varepsilon_L$ creep strain limit are obtained using the original laboratory oedometer data ($t_0$=1day), using Yin (1999)'s method. The permeability change parameter $c_k$ is adopted as $0.5e_0$ (Tavenas et al., 1983). The variations of ground water level are considered by setting different constant values in three different stages for simplicity. Construction of the embankment was finished in four days and in-situ monitoring was continued within a test period of 1000 days.

The embankment is a circular area and is simulated using axisymmetric model. The FE analysis is carried out as a coupled consolidation analysis of excess pore pressure dissipation and elastic viscoplastic deformation. The geometry of numerical model before and after deformation is shown in Fig. 2, in which there are five measuring points in different depths at the centre of embankment. The largest settlements can be observed in the clay layer under the centre of the embankment, where the strain condition is similar to one-dimensional.

Fig. 3 shows the calculation results of deformation and excess pore pressure in different depths of the ground. It can be concluded that the EVP model can predict the deformation and excess pore pressure of clay with high accuracy, especially the former ones. Some local inaccurate points are possibly due to the non-homogeneity inside the clay layer, since average values of parameters are adopted for the whole layer.

**Table 1** Soil parameters used for the clay layer under Berthierville embankment

| $\kappa$ | $\lambda$ | $\psi_0$ | $\Delta\varepsilon_L$ | $e_0$ | $k_0$ (m/d) | POP (kPa) | $\Phi'$ | $c'$ (kPa) | $\theta$ |
|---|---|---|---|---|---|---|---|---|---|
| 0.025 | 0.52 | 0.025 | 0.06 | 1.53 | 0.00026 | 6 | 30° | 1 | 0.5 |

**Table 2** Thickness and unit weights of the materials

| | Fill material | Topsoil | Fine to medium sand | Clay |
|---|---|---|---|---|
| $H$ (m) | 2.4 | 0.15 | 2.05 | 3.13 |
| $\gamma_{\text{saturated}}$ (kN/m$^3$) | 22 | 20 | 19.7 | 18 |
| $\gamma_{\text{unsaturated}}$ (kN/m$^3$) | 17 | 16 | 16 | 15 |

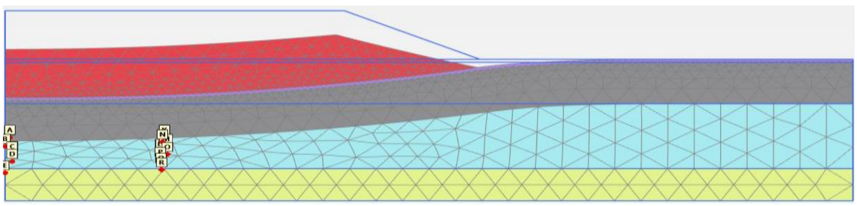

**Fig. 2** The geometry of the numerical model (the blue borders represent the undeformed geometry and the deformation is scaled up by 5 times)

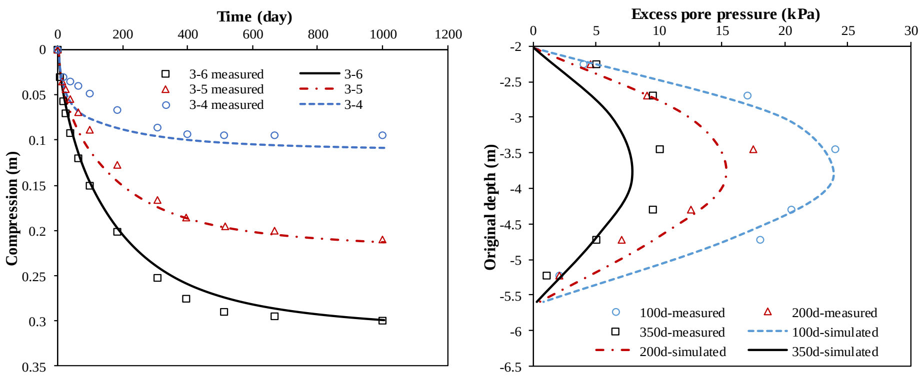


(a) (b)

**Fig. 3** The simulation results of (a) settlements and (b) excess pore pressure compared with measured data

### 3.2 The parametric study on the creep strain limit

Proper soil parameters are essential in finite element simulations, especially the creep parameters, which require oedometer test data for a certain test duration. Conventional creep models usually adopt a constant secondary coefficient fitted by 3 to 7-day's $\varepsilon$-ln($t$) curves (referred to as "linear model"). However, the $\varepsilon$-ln($t$) curves exhibit a nonlinear property (Yin, 1999) under long duration. For the Berthierville embankment, long-term creep tests had been conducted for up to nearly one year. Although the creep coefficients used in this study are fitted from the full curve, it is found that even 14-day's data produce similar results. Table 3 shows the creep parameters used for the parametric study, in which different values of $\Delta\varepsilon_L$ are used in the nonlinear creep model. For the linear model, $\Psi$ is fitted from 7-day's data. The linear creep is implemented in two ways: 1) by setting $\Delta\varepsilon_L$ as 100; 2) by using the Soft Soil Creep (SSC) model in Plaxis.

Fig. 4 shows the results of simulations with different sets of parameters. Firstly, the creep model has significant effects on the simulation. Conventional linear creep models (SSC) tend to overestimate the settlements of clay, especially after a long-time. Secondly, the selection of $\Delta\varepsilon_L$ influences the analysis results. A smaller value of $\Delta\varepsilon_L$ will underestimate the deformation while higher ones will overestimate that.

**Table 3** The creep parameters used for the clay in the parametric study

| Model | EVP in this study | | | | SSC |
|---|---|---|---|---|---|
| $\Delta\varepsilon_L$ | 0.02 | 0.06 | 0.1 | 100 | - |
| $\Psi_0$ *or* $\Psi$ | 0.025 | 0.025 | 0.025 | 0.02 | 0.02 |

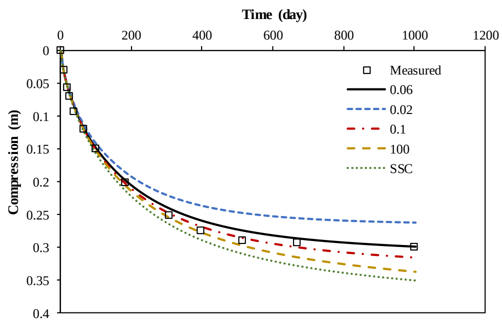


**Fig. 4** The comparison of clay compression with different creep models and values of $\Delta\varepsilon_L$

## 4 Conclusions

This paper presents the theory and algorithm of a 3-D elastic viscoplastic model based on Yin (1999)'s nonlinear creep equation for numerical analysis. Finite element analysis with the model is conducted in Plaxis for the clayey soil under Berthierville embankment. The results of settlement and excess pore pressure indicated the EVP model's capability in finite element simulations for clayey soils in field. A parametric study on the creep strain limit has also been carried out, which clearly shows the importance of long-term creep tests and parameter determination for the EVP model in this study.

**Acknowledgements**

The work in this paper is supported by a Theme-based Research Scheme (TRS) (Grant No.: T22-502/18-R) from Research Grants Council (RGC) of Hong Kong Special Administrative Region Government (HKSARG) of China and one GRF project (PolyU PolyU 152209/17E) from RGC of HKSARG of China. The authors also acknowledge the financial supports from Research Institute for Sustainable Urban Development of The Hong Kong Polytechnic University, and grants (BBAG, RBCN, ZDBS) from The Hong Kong Polytechnic University.

## References

Bjerrum, L. (1967). Engineering geology of Norwegian normally-consolidated marine clays as related to settlements of buildings. *Geotechnique*, *17*(2), 83-118.

Feng, W. Q., Li, Y. L., Yin, J. H., & Yin, Z. Y. (2014). The numerical implementation of elastic visco-plastic model for soft clays. *Numerical Methods in Geotechnical Engineering*, 39.

Kabbaj, M., Tavenas, F., & Leroueil, S. (1988). In situ and laboratory stress–strain relationships. *Geotechnique*, *38*(1), 83-100.

Perzyna, P. (1966). Fundamental problems in viscoplasticity. In *Advances in applied mechanics* (Vol. 9, pp. 243-377). Elsevier.

Tavenas, F., Leblond, P., Jean, P., & Leroueil, S. (1983). The permeability of natural soft clays. Part I: Methods of laboratory measurement. *Canadian Geotechnical Journal*, *20*(4), 629-644.

Yin, J. H., & Graham, J. (1989). Viscous–elastic–plastic modelling of one-dimensional time-dependent behaviour of clays. *Canadian Geotechnical Journal*, *26*(2), 199-209.

Yin, J. H. (1999). Non-linear creep of soils in oedometer tests. *Geotechnique*, *49*(5), 699-707.

Yin, J. H., Zhu, J. G., & Graham, J. (2002). A new elastic viscoplastic model for time-dependent behaviour of normally and overconsolidated clays: theory and verification. *Canadian Geotechnical Journal*, *39*(1), 157-173.

Yin, Z. Y., Chang, C. S., Karstunen, M., & Hicher, P. Y. (2010). An anisotropic elastic–viscoplastic model for soft clays. *International Journal of Solids and Structures*, *47*(5), 665-677.